Preprints of the 19th World Congress
The International Federation of Automatic Control
Cape Town, South Africa. August 24-29, 2014

Online Algebraic Identification of the Payload Changes in a Single-Link Flexible Manipulator Moving under Gravity

Andres San-Millan Rodriguez, Juan Carlos Cambera Ibañez, Vicente Feliu Battle.

Department of Electrical, Electronic and Automatic Control Engineering,University of Castilla-La Mancha, Ciudad Real, Spain (e-mail: Andres.SanMillan@uclm.es, JuanCarlos.Cambera@uclm.es,Vicente.Feliu@uclm.es).

Abstract: This paper presents a method for the on-line identification of the payload carried by a single-link flexible manipulator whose movement is constrained to the vertical plane. The vertical movement of the robot makes the effect of gravity not negligible, and determines therefore, the non-linear behaviour of the analysed system. The proposed estimator is based on the algebraic derivative approach in the frequency domain. The short period of time it takes for the algorithm to make an estimate, and its low computational burden make it suitable for real-time and adaptive control applications. The proposed estimator is experimentally tested in several situations carefully chosen to reproduce routine operations of the flexible manipulator.

Keywords: Flexible Robot, Estimation Parameters, Algebraic Estimator, On-line Algorithm.

1. INTRODUCTION

In the last decades, flexible link manipulators have drawn great attention because of its promising advantages over rigid manipulators. Building this type of robots do not only lead to potential building cost reductions but also has a positive impact on power consumption, maneuverability, weight, operational speed, operational security, among others(Dwivedy and Eberhard, 2006). All these advantages are achieved at the expense of the introduction of undesired vibrations, that reduce the robot accuracy. To overcome this disadvantage, great efforts have been carried out on the sensor development, kinematic and dynamics modelling, and control strategies, but many issues are still open(Benosman and Le Vey, 2004; Dwivedy and Eberhard, 2006).

The flexible link robots were born in the seventies through a NASA research program. The goal was reducing the launching cost of spacecrafts into orbit by creating lighter and more compact manipulators (W.J.Book, 1974). Since those studies, numerous earth applications have been developed based on these robots. In search and rescue applications, for instance, these robots are especially attractive as they reduce the power consumption and the overall weight of the platform, two desirable characteristics in a mobile robot. The Gryphon robot is a good example of these type of application. It consists on a four wheeled vehicle with a very long and lightweight arm used for demining tasks (Freese et al., 2007). In industry, the accurate positioning of the payload is usually a time consuming and sometimes risky task due to the highly flexible nature of bridge and gantry cranes. Applying the same control algorithm used to suppress vibrations on flexible robots, the operational effectiveness of cranes has been significantly improved (see an example on Sorensen et al. 2007).

When a flexible link robot performs pick and place tasks, the vibration frequencies of the robot are modified by changes in the payload, these changes of frequency, represent a serious problem which avoids the proper operation of the control scheme. Control algorithm parameters are tuned considering a fixed and known payload. When these parameters mismatch with the real payload, the algorithm reduces its accuracy, becomes less effective in suppressing vibration and, in some cases, may become unstable. Implementing an adaptive control law, to quickly adjust the control parameters, mitigates the aforementioned problems. However, it requires an on-line fast estimation of the payload.

Computational efficiency and fast convergence are usual requirements for on-line estimation, therefore the proposed estimator is based on the algebraic framework originally proposed in Fliess and Sira-Ramírez (2003). This algebraic method has been already used for fast identification of constant parameter in linear systems ranging from dc motors and servomotors to flexible manipulators.

The algebraic method has already been used for the estimation of parameters of DC motors by Mamani et al. (2008) and for servomotors by Garrido and Concha (2013), and for the estimation of the parameters of flexible manipulators by Pereira et al. (2011) and by Becedas et al. (2007). But we should mention that, in all the aforementioned works the identified systems were linear.

⋆ This study was financially supported by the Spanish Ministry of Economy and Competitiveness and by the European Social Fund with projects DPI2009-09956 and DPI2012-37062-CO2-01. It was also sponsored by the Spanish FPU12/00984 Program (Ministerio de Educacion, Cultura y Deporte)

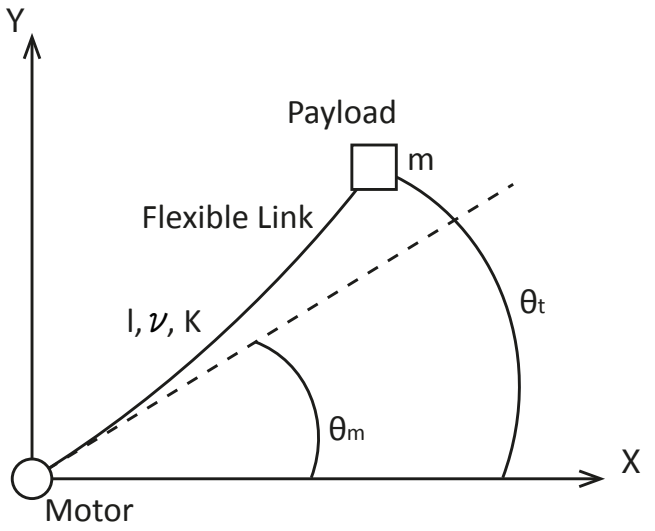

Fig. 1. Robotic system scheme

The estimator proposed in this work does not only provide estimates of the payload of the robot in a short period of time, but also the estimates are computed on-line due to the low computational burden of the developed algorithm. We should note that unlike previous works, where only linear systems are studied, the proposed estimator is specifically designed to work with our non-linear platform, which is a flexible robot whose movement is constrained to the vertical plane and where the effects of gravity are not negligible. This works complements the previous one of Becedas et al. (2007), where only a horizontal movement is considered.

This paper is organized as follows. Section 2 introduces briefly the dynamic model of the flexible arm. Section 3 is devoted to the design of the Algebraic Identification Algorithm. A description of the platform, experimental results and results analysis are presented in Section 4. Finally, Section 5 presents some conclusions and future work.

2. DYNAMIC MODEL

The flexible link robot under consideration is shown in Fig. 1. It consists mainly of an electrical rotary actuator and a slender beam, which holds an end-point payload. The base-end beam is clamped to the rotary hub of the actuator, which is responsible for moving the arm in a vertical plane. The dynamic model of the whole system can be expressed in two coupled subsystems, the actuator dynamics and, strictly speaking, the flexible link dynamics. For the purpose of the identification algorithm synthesis, only the flexible link dynamics model is relevant. It is exposed in the succeeding paragraphs.

The flexible link dynamics model relates the actuator position(θ_m) to the torque at the base of the beam (Γ) to the tip position of the beam (θ_t). The following model considers a massless beam with a point mass situated in its tip (payload). All the beam movements are in a vertical plane and, therefore, are affected by the gravitational force. It is also assumed that the only sources of potential energy are the bending of the beam and the gravitational force acting on the payload. Torsion and compression effects of the beam were not taken into account. Considering all these hypothesis, and the Euler-Bernoulli beam theory, as explained in **?**, the following dynamic model is found

$$c\left(\theta_m(t)-\theta_t(t)\right)=ml^2\ddot{\theta}_t(t)+\nu\dot{\theta}_t(t)+mgl\cos\left(\theta_t(t)\right) \tag{1}$$

where c is the link stiffness constant, m is the tip mass, ν is the beam viscous damping coefficient, l is the beam length, and g the gravitational constant. The stiffness constant of the beam could be expressed in terms of its length, its Young module (E) and its cross-sectional moment of inertia as follows

$$c=\frac{3EI}{l} \tag{2}$$

Moreover, a relation between the link deflection $(\theta_m-\theta_t)$ an the torque at the base of the link can be established as

$$c\left(\theta_m(t)-\theta_t(t)\right)=\Gamma(t) \tag{3}$$

The measurements available in the experimental platform are the angular position of the motor (θ_m) and the torque measured at the base of the link (Γ). It is not practical to measure the tip position (θ_t) because it usually requires expensive sensors, and these sensors may fail, for example because of occlusions. However, θ_t is necessary in order to carry out our estimation algorithm. Then the angular position of the tip of the robot is estimated using (3) in the following way

$$\theta_t^e(t)=\theta_m(t)-\Gamma(t)/c \tag{4}$$

Notice that θ_t^e, the estimation of the angular position of the tip, is independent of the payload mass. By substituting (3) in (1) and, using the θ_t^e as calculated above we obtain

$$\Gamma(t)=ml^2\ddot{\theta}_t^e(t)+\nu\dot{\theta}_t^e(t)+mgl\cos\left(\theta_t^e(t)\right) \tag{5}$$

3. IDENTIFICATION ALGORITHM

The algebraic methodology described in Fliess and Sira-Ramírez (2003) and in Becedas et al. (2007) is applied in this section to design real-time estimations of the tip mass m expressed in (5).

The Laplace transform of (5) is given by

$$\begin{aligned}\Gamma(s)=&ml^2\left[s^2\theta_t^e(s)-s\theta_t^e(0)-\dot{\theta}_t^e(0)\right]+\\&\nu\left[s\theta_t^e(s)-\theta_t^e(0)\right]+mgl\chi(s)\end{aligned} \tag{6}$$

being $\chi(s)$ the Laplace transform of $\cos\left(\theta_t^e(t)\right)$. If expression (6) were differentiated two times with regard to variable s, the initial conditions $\theta_t^e(0)$ and $\dot{\theta}_t^e(0)$ would be removed, yielding the expression

$$\frac{d^2\Gamma(s)}{ds^2} = ml^2\left[2\theta_t^e(s) + 4s\frac{d\theta_t^e(s)}{ds} + s^2\frac{d^2\theta_t^e(s)}{ds^2}\right] + \nu\left[2\frac{d\theta_t^e(s)}{ds} + s\frac{d^2\theta_t^e(s)}{ds^2}\right] + mgl\frac{d^2\chi(s)}{ds^2} \quad (7)$$

If expression (7) is multiplied by the factor s^2 (which represents two iterated integrations in the time domain), then an expression free of terms containing positive powers of the complex variable s can be obtained (positive powers of s must be avoided because they represent undesired repeated time differentiations of the signals involved). An expression involving only time convolutions of the signals $\Gamma(t)$, $\theta_t^e(t)$, and $\cos(\theta_t^e(t))$ is therefore yielded

$$s^{-2}\frac{d^2\Gamma(s)}{ds^2} = ml^2\left[2s^{-2}\theta_t^e(s) + 4s^{-1}\frac{d\theta_t^e(s)}{ds} + \frac{d^2\theta_t^e(s)}{ds^2}\right] + \nu\left[2s^{-2}\frac{d\theta_t^e(s)}{ds} + s^{-1}\frac{d^2\theta_t^e(s)}{ds^2}\right] + mgls^{-2}\frac{d^2\chi(s))}{ds^2} \quad (8)$$

Let us $\mathcal{L}$ denote the usual operational calculus transform acting on exponentially bounded signals with bounded left support. Recall that $\mathcal{L}^{-1}s(\cdot) = d/dt(\cdot)$, $\mathcal{L}^{-1}1/s(\cdot) = \int_0^t(\cdot)(\sigma)d\sigma$, and $\mathcal{L}^{-1}d^v/ds^v(\cdot) = (-1)^v t^v(\cdot)$. Expression (8) can thus be written in the time domain as follows [1]

$$\int^{(2)} t^2\Gamma(t) = ml^2\left[2\int^{(2)}\theta_t^e(t) - 4\int t\theta_t^e(t) + t^2\theta_t^e(t)\right] + \nu\left[-2\int^{(2)} t\theta_t^e(t) + \int t^2\theta_t^e(t)\right] + mgl\int^{(2)} t^2\cos(\theta_t^e(t)) \quad (9)$$

Expression (9) can be written in a compact form as

$$q(t) = m\left[l^2\beta(t) + gl\xi(t)\right] + \nu\eta(t) \quad (10)$$

where $q(t)$, $\beta(t)$, $\xi(t)$, and $\eta(t)$ can be calculated in real time because they are the outputs of the following time-varying linear, unstable, Brunovsky filters

$$\begin{aligned} q(t) &= z_1 & \xi(t) &= z_5 \\ \dot{z}_1 &= z_2 & \dot{z}_5 &= z_6 \\ \dot{z}_2 &= t^2\Gamma(t) & \dot{z}_6 &= t^2\cos(\theta_t^e(t)) \\ \beta(t) &= z_3 + t^2\theta_t^e(t) & \eta(t) &= z_7 \\ \dot{z}_3 &= z_4 - 4t\theta_t^e(t) & \dot{z}_7 &= z_8 + t^2\theta_t^e(t) \\ \dot{z}_4 &= 2\theta_t^e(t) & \dot{z}_8 &= -2t\theta_t^e(t) \end{aligned} \quad (11)$$

whose initial states are set to zero.

[1] We denote by $(\int^{(j)}\phi(t))$ the integral expression $\int_0^t\int_0^{\sigma_1}\cdots\int_0^{\sigma_{j-1}}\phi(\sigma_j)d\sigma_j\ldots d\sigma_1$ with the definition of $(\int\phi(t))$ as $(\int_0^{(1)}\phi(t)) = \int_0^t\phi(\sigma_1)d\sigma_1$

The linear equation (10) has two unknowns, m and ν, which can be obtained from a least squares error fitting in the time interval $[t_i, t_f]$ between the first and the last available sample. Upon defining a cost:

$$\varepsilon = \int_{t_i}^{t_f}\left\{\left[\, l^2\beta(\tau) + gl\xi(t) \;\; |\eta(\tau)\,\right]\cdot\begin{bmatrix} m \\ \nu\end{bmatrix} - q(\tau)\right\}^2 d\tau, \quad (12)$$

its minimization leads to

$$\begin{bmatrix} m \\ \nu\end{bmatrix} = \left[\int_{t_i}^{t_f}\begin{bmatrix} l^2\beta(\tau) + gl\xi(\tau) \\ \eta(\tau)\end{bmatrix}\begin{bmatrix} l^2\beta(\tau) + gl\xi(\tau) \\ \eta(\tau)\end{bmatrix}^T d\tau\right]^{-1}\cdot\int_{t_i}^{t_f}\begin{bmatrix} l^2\beta(\tau) + gl\xi(\tau) \\ \eta(\tau)\end{bmatrix} q(\tau)d\tau \quad (13)$$

Here, only the positive solutions for m and ν have physical sense, and for the purposes of this work, only the value of m is relevant.

Before finishing this section, it is important to mention that, because of the unstable nature of the Brunovsky filters, this identification procedure requires periodically resets to avoid reaching the numerical limits in the computer. Faster reset actions should be considered to detect sudden payload changes, as long as this algorithm is only capable of perform an unique payload estimation. This last remark becomes evident from the equation (11). In this equation, the functions $q(t)$, $\beta(t)$, $\xi(t)$ are calculated by the integration of the sensor measurements, and they have, as therefore, memory. Considerations about resetting this type of identification algorithm has been already discussed in San-Millan and Feliu (2014), and will not be covered in this paper.

4. EXPERIMENTS

This section presents the experiments carried out to verify the estimation algorithm developed.

4.1 Experimental Platform

The identification algorithm exposed in this paper was tested in a single-link flexible robot built in our laboratory, and showed in Fig. 2.

Its mechanical structure consists of a Maxon DC motor with a gear reduction, a duraluminium link connected to the gear shaft, and a mass-adjustable payload structure. A Maxon EPOS driver controls the motor position, while a National Instruments PXI system allows us to command the motor driver and to register the sensory signals. The sensory system is composed of a strain-gage structure placed at the base of the arm, and two rotary encoders mounted to the shaft of the motor and to the output shaft of the reduction gear. The strain-gage structure provides an estimate of the actuator output torque (Γ). Two encoders were installed because of the presence of backlash in the gear reduction. The outer encoder measures the exact orientation of the beam base (θ_m). The inner encoder was not taken into account in our experiments.

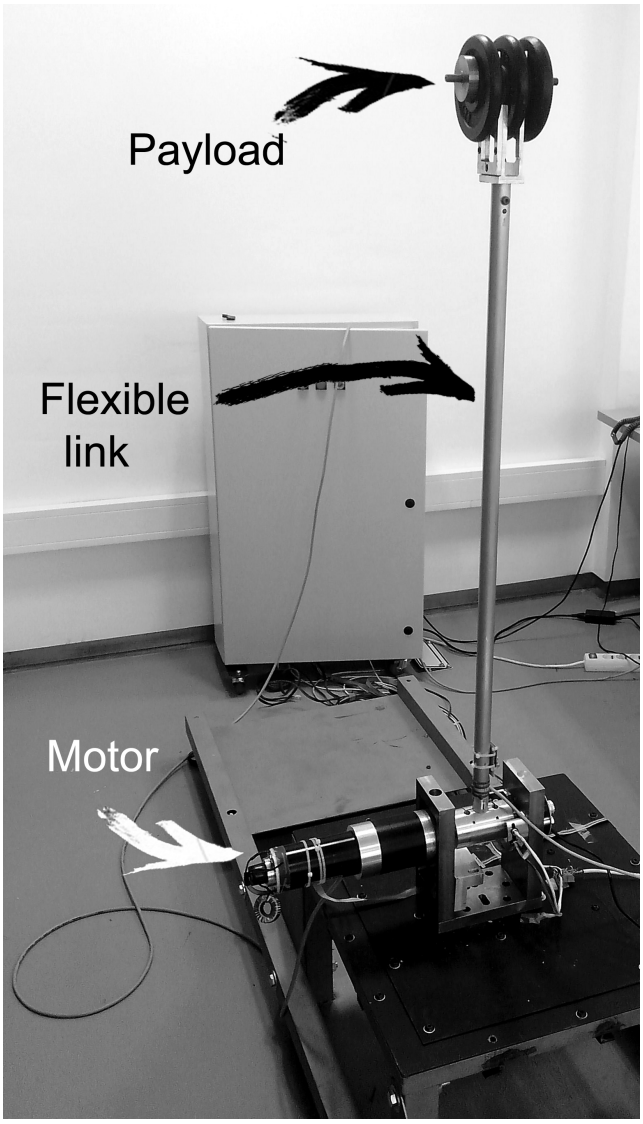

Fig. 2. Flexible single-link robot platform

The most relevant parameters of the platform, in relation to the experiments, are summarized in table 1.

Table 1. flexible robot parameters

Parameter	Units	Symbol	Value
Beam length	(m)	l	1.045
Beam rotational stiffness	(N.m.rad^{-1})	c	2498.2
Beam viscous damping coefficient	(N.m.s.rad^{-1})	ν	0.2
Payload mass 1	(Kg)	m_1	1.150
Payload mass 2	(Kg)	m_2	1.690
Payload mass 3	(Kg)	m_3	2.930

4.2 Experimental Results

In order to validate the proposed identification algorithm, three types of experiments were carried out for three different payloads (m_1,m_2 and m_3), whose values are shown in table 1. In these experiments, the algebraic controller presented in Cambera et al. (2014) was considered to control the motor position, while no controller was used to control the tip position. In any case, it is important to point out that the results presented in this paper do not depends on the motor control algorithm, but only on the motor position and the torque measurements. A description of each type of experiment is given below.

Experiment type 1. The motor position (θ_m) follows a fourth-order trajectory that goes from 90 to 45 degrees in 2 seconds. This experiment reproduces the typical task of picking up an object and position it on another place following a certain trajectory. It is worth noting that even when in practice a pick-up position of 90 degrees does not make sense, from the experimental validation standpoint does it. This starting position allows us to easily recreate the situation in which the robot has no payload mass (zero torque), and then it picks up an object which is on a surface.

Experiment type 2. The motor position (θ_m) follows a sinusoidal trajectory that goes from 90 to 45 degrees with a period of 4 seconds, and considering a trapezoidal velocity profile. This experiment allows us to prove that the algorithm does not become unstable when a persistent input is applied. This conclusion is not obvious considering that the estimation algorithm is based on unstable Brunovsky filters.

Experiment type 3. The motor is fixed to 0 degrees ($\theta_m = 0$), and then the flexible link is kindly hit with a hammer in its tip. Through this experiment we recreate two case-scenarios. In the first case, the robot is initially at rest under an external disturbation. In the second one, we suppose that the algorithm that controls the robots does not cancel entirely the residual vibrations.

For each experiment type, we present a figure that plots sensor measurements, and another one with the estimation output. Due to space limitations, we only present the sensor measurements for the payload mass m_2. The graphics for payload masses m_1 and m_3 are quite similar, and do not add relevant information to the analysis of results. At the end of this section, a summary table shows the convergence rates of the estimation algorithm.

Results of experiments type 1. In Fig. 3, we present the motor position and torque measurement for mass m_2. Then, Fig. 4 shows the identification algorithm behavior for all the masses.

Results of experiments type 2. In Fig. 5, we present the motor position and torque measurement for mass m_2. Then, Fig. 6 shows the identification algorithm behavior for all the masses.

Results of experiments type 3. In Fig. 7, we present the motor position and torque measurement for mass m_2. Then, Fig. 8 shows the identification algorithm behavior for all the masses.

Table 2 summarizes the time elapsed from the start of the algorithm until it estimates the payload mass with an error less than 10%, 5% and 2%.

Table 2. Comparison of convergence time between different experiments and payloads

	Experiment 1			Experiment 2			Experiment 3		
Errors	10%	5%	2%	10%	5%	2%	10%	5%	2%
Payload m_1	0.57 s	0.77 s	1.08 s	0.68 s	0.84 s	1.24 s	0.022 s	0.028 s	0.030 s
Payload m_2	0.33 s	0.61 s	1.27 s	0.40 s	0.65 s	0.88 s	0.036 s	0.132 s	0.238 s
Payload m_3	0.29 s	0.39 s	0.58 s	0.58 s	0.73 s	1.16 s	0.048 s	0.050 s	0.196 s

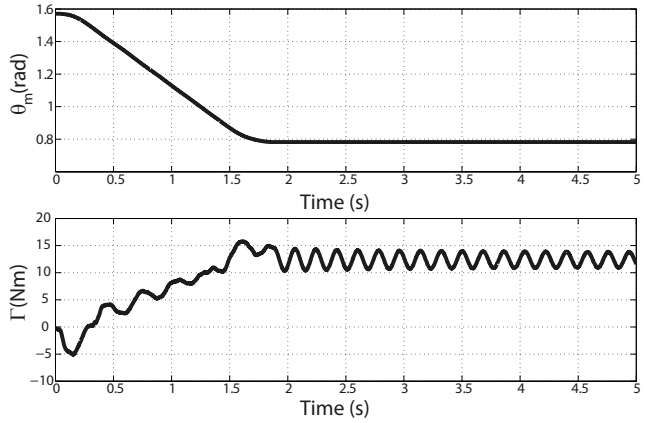

Fig. 3. Experiment type 1: Motor position and torque measurement for mass m_2

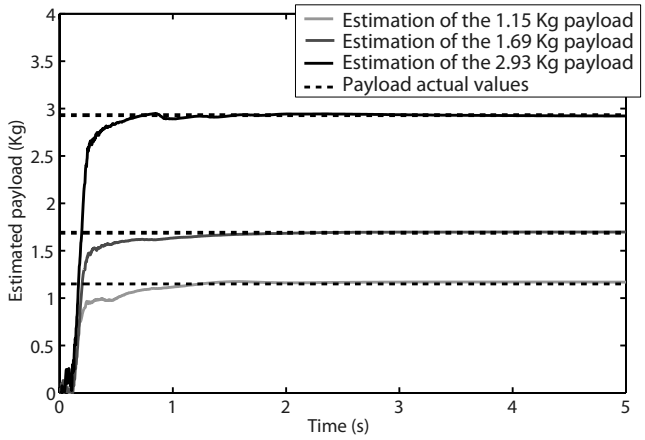

Fig. 4. Experiment type 1: Payload mass estimation

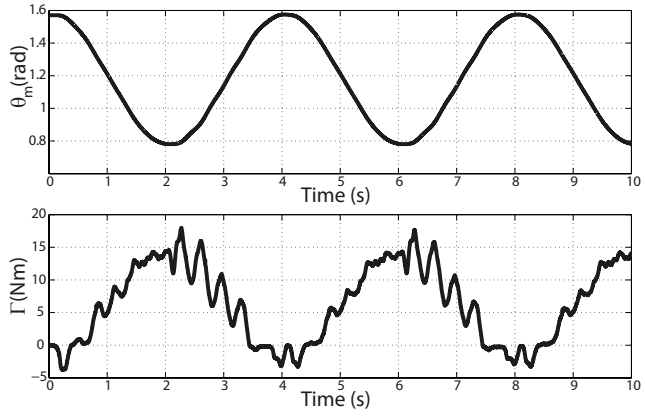

Fig. 5. Experiment type 2: Motor position and torque measurement for mass m_2

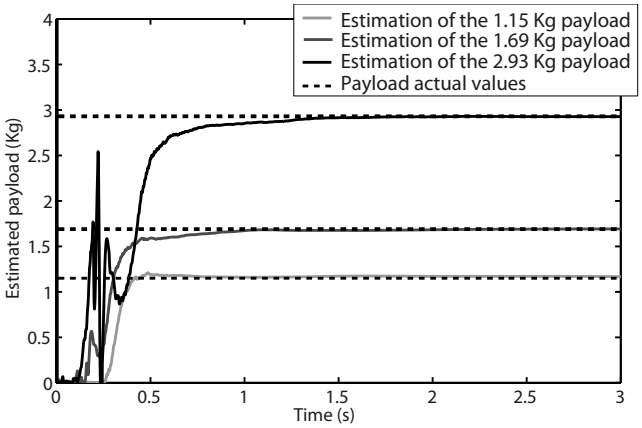

Fig. 6. Experiment type 2: Payload mass estimation

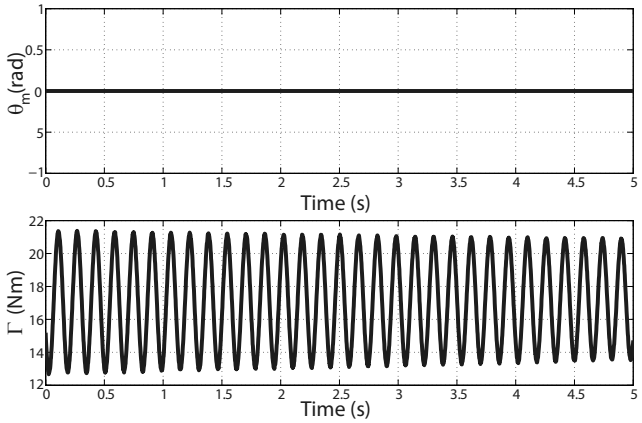

Fig. 7. Experiment type 3: Motor position and torque measurement for mass m_2

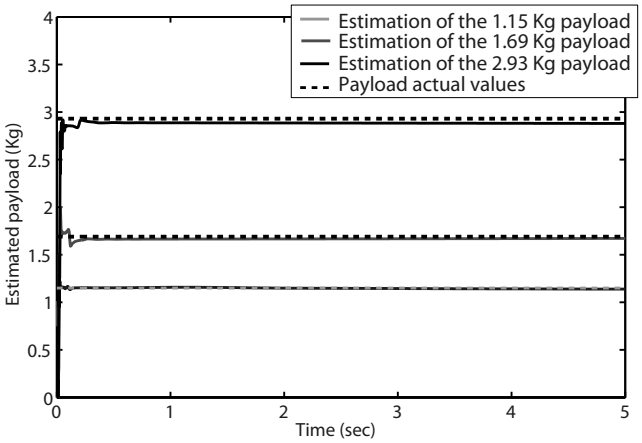

Fig. 8. Experiment type 3: Payload mass estimation

4.3 Analysis of the Experimental Results

From the perspective of adaptive control, an estimation algorithm must be able to ensure a correct and fast estimation for the typical operation circumstances of the system. It would be also desirable that the estimates were carried out with a known and invariant rate of convergence. In the following paragraphs we discuss the Experimental Results in this context.

Considering the figures shown in the previous section, it can be seen that the proposed algorithm fulfills the first requirement (producing accurate and fast estimates). According to the data in table 2, our algorithm is able to estimate the payload mass in less than 0.85 seconds with a error below 5%. This means that the algorithm performs well in those situations where large trajectories are involved (experiments type 1 and 2), and also under quasistatic situations (experiment type 3). It is important to mention that the algorithm stays stable under persistent inputs (experiment type 2) despite it is based on unstable filters. From a more general point of view, these results indicate that once the control algorithm adjusts its parameters, it still has one half of the trajectory to improve the tracking and to cancel any existing vibration.

In terms of the rate of convergence variance, there are greater differences between certain experiments. In the experiments which involve large trajectories (experiments type 1 and 2), the estimation of the tip mass has been carried out in an average time of 0.48, 0.67 and 1.03 seconds with an error of 10%, 5% and 2%, showing a small variance in each case . Meanwhile in the quasistatic situation (experiment type 3), the algorithm has spent 0.035, 0.07 and 0.15 seconds to calculate the payload mass with 10%, 5% and 2% errors. In other words, in the quasistatic situation the algorithm was about 8 times faster than when large trajectories were involved. From these observations, we conclude that two convergence rates should be taken into account in the control algorithm design (large trajectories and quasistatic situations). Fortunately, these situations are very different.

5. CONCLUSIONS

An on-line identification algorithm, based on the algebraic method, has been designed for the quick payload mass estimation of a flexible link arm moving under gravity. This algorithm only requires the motor position and torque at the base of the flexible link. In contrast to other methodologies, this one does not require any signal derivation, and therefore, noise amplification in the sensor measurements is avoided.

The experimental validation shows, that for typical trajectories of a robot arm of such dimensions (45 degrees in 2 seconds), the identification algorithm is capable of making an estimate in less of 0.85 seconds with only 5% of error. Adjusting the parameters of a control algorithm with this payload estimation should be enough to cancel effectively the vibrations and to improve the tracking in the second half of the trajectory. For quasistatic situations, when the joint remains motionless but the link slightly vibrates, the payload estimation can be performed about 8 times faster. Further work will focus on designing an adaptive control law based on the estimation algorithm here presented. Experimental validation will be also carried out.

REFERENCES

Becedas, J., Trapero, J., Sira-Ramirez, H., and Feliu-Battle, V. (2007). Fast identification method to control a flexible manipulator with parameter uncertainties. In *Robotics and Automation, 2007 IEEE International Conference on*, 3445–3450. doi: 10.1109/ROBOT.2007.364005.

Benosman, M. and Le Vey, G. (2004). Control of flexible manipulators: A survey. *Robotica*, 22(5), 533–545.

Cambera, J.C., Chocoteco, J.A., and Feliu, V. (2014). Feedback linearizing controller for a flexible single-link arm under gravity and joint friction. In *ROBOT2013: First Iberian Robotics Conference*, 169–184. Springer.

Dwivedy, S.K. and Eberhard, P. (2006). Dynamic analysis of flexible manipulators, a literature review. *Mechanism and machine theory*, 41(7), 749–777.

Fliess, M. and Sira-Ramírez, H. (2003). An algebraic framework for linear identification. *ESAIM Control Optimisation and Calculus of Variations*, 9, 151–168. doi:10.1051/cocv:2003008.

Freese, M., Matsuzawa, T., Oishi, Y., Debenest, P., Takita, K., Fukushima, E.F., and Hirose, S. (2007). Robotics-assisted demining with Gryphon. *Advanced Robotics*, 21(15), 1763–1786.

Garrido, R. and Concha, A. (2013). An algebraic recursive method for parameter identification of a servo model. *IEEE/ASME Transactions on Mechatronics*, 18(5), 1572–1580. doi:10.1109/TMECH.2012.2208197.

Mamani, G., Becedas, J., and Feliu-batlle, V. (2008). Online fast algebraic parameter and state estimation for a dc motor applied to adaptive control.

Pereira, E., Trapero, J.R., Muñoz D'í'az, I., and Feliu-Batlle, V. (2011). Algebraic identification of the first two natural frequencies of flexible-beam-like structures. *Mechanical Systems and Signal Processing*, 25(7), 2324–2335. doi:10.1016/j.ymssp.2011.03.007.

San-Millan, A. and Feliu, V. (2014). A fast online estimator of the two main vibration modes of flexible structures from biased and noisy measurements. *Mechatronics, IEEE/ASME Transactions on.* doi: 10.1109/TMECH.2014.2304302.

Sorensen, K.L., Singhose, W., and Dickerson, S. (2007). A controller enabling precise positioning and sway reduction in bridge and gantry cranes. *Control Engineering Practice*, 15(7), 825–837.

W.J.Book (1974). *Modeling, desing and control of flexible manipulators arms.* Ph.D. thesis, Massachusetts Institute of Technology, Dept. of Mechanical Engineering.